HATs meet structural biology

Josep Rullo-Tubau[1], Paola Bartoccioni[1,2], Oscar Llorca[3], Ekaitz Errasti-Murugarren[1,2,4] and Manuel Palacín[1,2,5]

1) Institute for Research in Biomedicine, The Barcelona Institute of Science and Technology (BIST). Baldiri i Reixac 10. E-08028 Barcelona, Spain.
2) The Spanish CIBER of Rare Diseases (CIBERER), ISCIII. U-731. E-08028 Barcelona, Spain.
3) Structural Biology Programme, Spanish National Cancer Research Centre (CNIO), Melchor Fernández Almagro 3, E-28029 Madrid, Spain.
4) Department of Physiological Sciences II. School of Medicine. University of Barcelona. Feixa Llarga (without number). E-08907 L'Hospitalet de Llobregat. Spain.
5) Department of Biochemistry and Molecular Biomedicine, Universitat de Barcelona, Spain.

Correspondence to be sent to: Manuel Palacín. Manuel.palacin@irbbarcelona.org

Abstract (3335 words from Introduction to acknowledgements)

Heteromeric amino acid transporters (HATs) are one of the ten types of amino acid transporters present in the human body. Growing interest in the pathophysiological role of this group of transporters in rare and complex diseases and cancer has brought about the recent resolution of various structures of human HATs and bacterial homologues at atomic level. This knowledge sheds light on the mechanisms of transport used by these molecules. Here we discuss the molecular bases underlying substrate specificity, binding asymmetry, and the impact of disease-causing mutations on transporter biogenesis and function.

Introduction

Amino acid transport across cell membranes regulates the intracellular amino acid content and is essential for cellular metabolism [1]. Heteromeric amino acid transporters (HATs) form disulfide-linked heterodimers composed of two polypeptides: a heavy or ancillary protein (SLC3 family, rBAT, and CD98hc), required for trafficking the holotransporter to the plasma membrane, and a light subunit (SLC7 family, L-type amino acid transporters or LAT) responsible for amino acid transport activity [2-4]. LATs are obligatory exchangers that confer substrate selectivity to the heterodimer, mediating the uptake of all common amino acids except proline.

Several human pathologies highlight the physiological relevance of HATs. In particular, mutations in these transporters have been associated with inherited rare or complex metabolic / neural disorders ($b^{0,+}$AT/rBAT, y^{+}LAT1/CD98hc, LAT1/CD98hc and LAT2/CD98hc) [2,5,6] while the overexpression of some members of this family (LAT1/CD98hc, xCT/CD98hc and LAT2/CD98hc) has been linked to tumor cell survival and progression, and chemoresistance [7-9]. Moreover, the glycine and D-serine transporter Asc1/CD98hc is a potential therapeutic target to modulate NMDA glutamate receptors in excitotoxicity and in pathologies involving the hypofunction of NMDA receptors [10-12]. Growing interest in the pathophysiological relevance of this group of transporters has led to the recent resolution of several atomic structures of human and mammalian HATs (LAT1/CD98hc, LAT2/CD98hc, xCT/CD98hc and $b^{0,+}$AT/rBAT) [13-21], and the bacterial LAT BasC [22], thus paving the way for the dissection of the molecular mechanisms underlying substrate specificity, as well as the impact of disease-causing mutations.

Architecture of HATs

The heavy subunits of HATs are type II membrane glycoproteins with a bulky extracellular domain (ED) with sequence and structural homology with members of the α-amylase family, a short segment (neck) connecting with the transmembrane domain (TM) 1', and a large cytosolic N-terminus [14,15,23]. CD98hc-ED has a $(\beta/\alpha)_8$-barrel fold domain (named A) followed by a β-sandwich domain (named C), whereas rBAT ectodomain has an additional domain (named B) in the loops between β3 (subdomain BI) and α3 and β4 and α4 (subdomain BII) within domain A.

HATs light subunits present the APC (Amino Acid-Polyamine-Organocation superfamily) fold, initially described for the bacterial amino acid transporter LeuT [24]. In particular, they have 12 TM domains, with TMs 1 and 6 unwound in the center, forming two discontinuous helices named TM1a and TM1b, and TM6a and TM6b, which host the substrate-binding site [13-15,19,22]. The pseudo two-fold symmetry, which relates TM1-TM5 and TM6-TM10, largely governs the rocking bundle-based substrate translocation mechanism in APC-fold transporters [25,26]. In this mechanism, tilting of the bundle domain (formed by TMs 1, 2, 6 and 7) over the hash domain (TMs 3, 4, 8, and 9) explains the major conformational changes during the inward- to outward-facing transition. Rearrangements of TMs 5 and 10 have also been suggested to play a role in the substrate translocation mechanism [22,27,28]. Finally, TMs 11 and 12 form a V-shape at the external side of TM10 facing the membrane lipids.

Currently solved structures of mammalian HATs and bacterial LATs are in inward-facing conformations, except for human LAT1/CD98hc bound to the inhibitor 3,5-diiodo-L-tyrosine, which was solved in an outward-facing/occluded state [16]. AlphaFold structural predictions of light subunits of HATs (https://alphafold.ebi.ac.uk/) [29] recapitulate the conformations already determined experimentally. Thus, structures of HATs in every state of the transport cycle are still missing.

The interaction between heavy and light subunits has common features in all the structures solved (Fig. 1A-B): i) a disulfide bond connects two conserved cysteine residues in the neck of the heavy subunit and the extracellular loop 2 (EL2), between TMs 3 and 4, in the light subunit; b) tight hydrophobic interactions in the membrane region connect TM1' in the heavy subunit with TM4 in the light subunit; and iii) in the cytoplasm, the N-terminal α-helix of the heavy subunit interacts with the C-terminal α-helix of the light subunit [13-15,19,22].

The ED of the heavy subunits is located above the light subunit (Fig. 1A) and also presents several polar interactions, in addition to the disulfide bond between the two subunits, connecting $(\beta/\alpha)_8$-barrel loops of the heavy subunit ED and extracellular loops of the light subunits. These connections and the relative position between the ED and the light subunits vary in the cryo-EM structures of human inward-facing LAT1/CD98hc, LAT2/CD98hc and xCT/CD98hc, and outward-facing/occluded LAT1/CD98hc; see description of these connections here [15,16,19,21]. Interestingly, the interaction of rBAT-ED and CD98hc-ED with its respective subunits shows clear differences [13-17,19-21]. The "neck" of rBAT (6 residues) is shorter than that of CD98hc (11 residues), thus changing the interaction with the globular ED and causing a relative displacement of ~40 Å in the relative position between the ED and the light subunit. Finally, the bottom surface of the rBAT-ED is mostly negatively charged [20], whereas that of 4F2hc-ED is positively charged [30], thus pointing to distinct electrostatic interactions. The functional relevance of these differences is currently unknown.

Cryo-EM revealed differences in the oligomeric state of several HATs, heterodimers being the CD98hc-associated transporters and superdimers (dimers of heterodimers) the $b^{0,+}$AT/rBAT transporters (Fig. 1A-B), thereby confirming previous biochemical studies [31]. Indeed, the superdimer interface implicates only residues in domains B and A of the rBAT-ED [15,17,20] (Fig. 1B). Cryo-EM structures of $b^{0,+}$AT/rBAT revealed a Ca^{2+} atom within domain B (Fig. 1B), suggesting that this cation stabilizes the two halves (subdomains BI and BII) of this domain [15,17,20].

Biogenesis

The biogenesis of HATs has been studied mostly for b^{0+}AT/rBAT [20,32-37]. For CD98hc and its light subunits, information is scarce and relative to the stabilization of the purified light subunit by CD98hc [38]. The light subunits and the corresponding heavy subunits depend on each other to reach the plasma membrane [20,32-35]. In this regard, in the absence of $b^{0,+}$AT, rBAT localizes in the endoplasmic reticulum (ER) as an Endo H-sensitive N-glycosylated protein, which is rapidly degraded, mainly through the ERAD pathway. In contrast, without rBAT, $b^{0,+}$AT remains much longer within the ER, and is most likely already folded [32]. Assembly with $b^{0,+}$AT occurs in the ER, facilitating the oxidative folding of rBAT-ED and preventing rBAT degradation. The disulfide bridge Cys^{571}–Cys^{666} and the N-glycan in Asn^{575}, located in domain C, are essential for trafficking to the Golgi apparatus to acquire N-glycan maturation [32,36,37].

Cryo-EM structures revealed that residues in domains B and A of rBAT-ED govern the oligomeric state (i.e., dimers of heterodimers or superdimers) (Fig. 1B) [15,17,20], each heterodimer being an independent transport unit [31]. This structural scenario facilitates an understanding of transporter biogenesis in health and disease, where the formation of superdimers would be key for the transit of the transporter to the Golgi apparatus [20,32]. The five cystinuria missense mutations of rBAT (L89P, T216M, M467T/K and R365W) more deeply studied show defective biogenesis when co-expressed with $b^{0,+}$AT in mammalian cells [20,32]. L89P is located in the TM1' domain (Fig. 2A), very close to the interacting segment of TM1' with TM4 of $b^{0,+}$AT, and to a cholesterol binding site that connects rBAT to TM4 of $b^{0,+}$AT (19). Mutation L89P will tilt the axis of the TM1´helix, compromising the interaction with cholesterol and with TM4 of $b^{0,+}$AT. Indeed, the L89P mutant dramatically decreases the formation of heterodimers with $b^{0,+}$AT and thus also of superdimers, and even though this minimal expression acquired mature glycosylation [20,32], this mutation causes a considerable loss of transport function in non-polarized and polarized cells overexpressing the transporter [20,32].

Mutation L89P suggests a role of cholesterol in the formation of heterodimers and the biogenesis of $b^{0,+}$AT/rBAT but direct experimental evidence is missing. Cholesterol stabilizes HATs, and thus steroid detergents (e.g., digitonin or GDN) or cholesterol addition during HATs purification has been used to solve all the HAT structures reported. In these structures, including $b^{0,+}$AT/rBAT solved in nanodiscs [20], several molecules of steroid detergents or cholesterol have been identified (Fig. 2A). Which molecules of cholesterol

have a role in the stability and biogenesis of $b^{0,+}$AT/rBAT and in other HATs is at present unknown.

Cryo-EM structures identified a Ca^{2+} atom bound between the subdomains BI and BII of rBAT-ED behind the rBAT homodimerization interface [15,17,20] (Fig. 2B). Mutational studies revealed that Ca^{2+} or a positive charged residue (e.g., mutation to lysine) mimicking Ca^{2+} is key for the formation of superdimers and traffic to the Golgi apparatus, as revealed by monitoring N-glycan maturation of rBAT. In contrast, mutations of Ca^{2+}-interacting residues, designed to weaken Ca^{2+} binding, block rBAT maturation and consequently amino acid transport at the cell surface [20]. Thr 216 is located near the Ca^{2+} atom, and mutation T216M does not affect heterodimerization with $b^{0,+}$AT, but blocks the formation of superdimers and rBAT maturation [20,32]. These studies support that proper folding of rBAT-ED, validated by formation of the superdimer, is key to exit the ER and reach the Golgi apparatus.

Arg 365 is located in helix α4 of domain A (Aα4), next to residue Arg 362, one of the residues connecting the superdimer (Fig. 2C), which would explain why the R365W mutation does not affect heterodimerization with $b^{0,+}$AT, but instead blockssuperdimer formation and maturation of rBAT, resulting in a decreased transport function at the cell surface [20,32]. The Met 467 mutants affect heterodimerization (M467T) and/or N-glycan maturation (M467K) and show no transport in transfected cells [20,32]. Met 467, within Aα7, is located in the interface with domain C [20], where relevant elements for N-glycan maturation of rBAT are present (Cys571–Cys666 and N-glycan Asn575) [32,36,37] (Fig. 2D). This observation suggests that Met 467 mutants affect the folding of rBAT-ED.

Unlike rBAT mutations, for those $b^{0,+}$AT mutations that have been studied, only G105R (localized in the very short cytoplasmic loop TM2-TM3) drastically reduces half-life of $b^{0,+}$AT (P. Bartoccioni, personal communication), protein expression and transport activity in cells overexpressing the two subunits [20,32]. Whether this mutation affects integration in the membrane has not been addressed.

Structural determinants of substrate selectivity

Solved structures of the light subunits of HATs and the bacterial BasC bound to substrates correspond to inward-facing conformations within the transport cyle (Fig. 3A). Moreover, human LAT1 bound to inhibitors and bacterial GkApcT bound to substrates have been

solved as variants of a fully occluded conformation (Fig. 3A). Thus, dissection of the structural determinants of substrate selectivity has been guided by this limited information within the transport cycle. Substrate selectivity in HATs is mediated primarily by interactions of the substrate α-amino and carboxyl moieties with residues comprising unwound segments of TM1 and TM6 [13-15,19,22] (Fig. 3B. The interacting residues in TM1 consist of the highly conserved GSG motif (the exceptions being the light subunits AGT1 and xCT presenting a GAG motif). In contrast, the residues in the unwound segment of TM6 are less conserved and play an important role in determining substrate specificity [8,15,18,21].

LAT1/CD98hc, LAT2/CD98hc and Asc1/CD98hc transport neutral amino acids but of different sizes. LAT1/CD98hc is specialized in large neutral amino acids but it is inefficient for L-glutamine uptake. LAT2/CD98hc transports both large and small neutral amino acids and it is highly efficient for L-glutamine. Finally, Asc1/CD98hc mediates the preferential uptake of small neutral amino acids [2,39-41]. Interestingly, a glycine or a serine residue within the unwound segment of TM6 regulates substrate selectivity [18]. Thus, LAT1/CD98hc and LAT2/CD98hc large substrates interact with the backbone carbonyl of glycine 246 (hLAT2 numbering), while a serine at the equivalent position (as in Asc1) is key for small neutral amino acid selectivity [18] (Fig.3A). Similarly, a negatively charged residue (Asp 233) in the equivalent position of the dibasic amino acid transporter $b^{0,+}$AT/rBAT contribute to this selectivity [20] by facilitating interaction with the positively charged side chain of the substrates [15] (Fig. 3C). $b^{0,+}$AT/rBAT also mediates the uptake of neutral amino acids [13-17,19-21,42], Asn 236 in TM6 (Fig. 3C) being identified by functional studies as a determinant for this substrate selectivity [20]. The role of TM6 in substrate selectivity appears to be a conserved mechanism in other transporter families with the APC fold, although with variations. Thus, residues in the unwound segment of TM6 or in TM6b determine substrate size in transporters of the SLC6 family of Na^+-dependent symporters for amino acids, neurotransmitters, osmolytes, and creatine [43,44]. However, substrate selectivity determinants of HATs are not found exclusively in TM6. For instance, Asn 134 (TM3) in human LAT2/CD98hc also plays a relevant role in the selectivity for small neutral amino acids, and when Asn 134 is mutated to the equivalent residue found in hLAT1/CD98hc (N134S), substrate selectivity changes diametrically, showing reduced transport of glycine, alanine and glutamine, thus mimicking the selectivity of LAT1/CD98hc [18].

Strikingly, xCT/CD98hc, which shows the most restricted substrate selectivity among human LATs [45], presents unorthodox binding poses for both glutamate and cystine [19]. Instead

of binding to the backbone residues of TM1 and TM6, glutamate is shifted away to TM3 and TM8 (Fig. 3D). For cystine, docking analysis predicted that the carboxylate in one end would interact simultaneously with residues in the unwound segment of TM1, and with Ser 330 in TM8. The α-amine of this cysteine half would interact with the backbone carbonyl of Tyr 244 (TM6). On the other cysteine half, the carboxylate seems to interact with Arg135 (TM3) and 396 (TM10), while the adjacent α-amine would interact with the backbone carbonyl of Gly 336 in TM8. Therefore, selectivity in xCT/CD98hc might be determined by its ability to accommodate the two negatively charged moieties of the substrate, a process in which Arg 135 and 396, unique to xCT/CD98hc, are essential [19]. Whether this particular substrate pose within the xCT/CD98hc binding site represents the canonical pose or an intermediate state is unknown at present.

xCT/CD98hc shows an induced-fit conformational change that is unique within HATs [19]. The binding of substrate glutamate facilitates the interaction between Tyr 251 (TM6) and Arg 135 (TM3) with the knock-on effect of TM8 transitioning from a partially unwound to a rigid helical state (Fig. 3C). Calculations performed with cystine also show an increase in rigidity in the region of TM8 neighboring the substrate, whereas the cytoplasmic end of this transmembrane segment remains disordered. The different behavior observed between glutamate and the larger cystine suggests that the conformational state of TM8 dynamically modulates the volume of the xCT/CD98hc binding site.

Substrate selectivity is determined not only by the identity of the amino acid residues themselves but also by the spatial conformation of the transmembrane domains. In this regard, interaction between TM2 and TM6 in human LAT2/CD98hc has been found to be a determinant of this transporter's ability to translocate small neutral amino acids and glutamine [18]. Indeed, mutation of Tyr 93 (TM2) to alanine disrupts the transport of glycine, alanine and glutamine, while having minimal effect on larger substrates such as tryptophan. Molecular dynamics suggest that this mutation in TM2 alters the conformation of TM6, which results in a widened gap between the unwound segments of TM1 and TM6. Small amino acids, lacking large side chains to establish additional interactions with neighboring residues, cannot therefore achieve the productive binding pose that results in decreased V_{MAX} with no alteration of K_M.

Asymmetrical interaction with substrates

A physiologically relevant characteristic of HATs is the asymmetry in apparent substrate affinity (i.e., K_M) at both the intracellular and extracellular sides of the transporter. This asymmetry allows HATs to regulate intracellular amino acid pools (mM concentrations) by exchange with external amino acids (μM concentration range) [46]. The molecular bases of substrate asymmetry rely on at least two distinct and fully conserved residues, which have been suggested to participate in both substrate interaction and conformational rearrangements upon substrate binding [22]. A conserved tyrosine in TM7, in an equivalent position to the Na1 in the sodium-dependent transporters with APC-fold, has been proposed to maintain the differential tension on the unwound segments of TM1 and TM6 in substrate-bound and apo states [22]. In fact, while this tyrosine residue interacts with both TM1 and TM6 in nearly all solved apo HAT and bacterial BasC structures, substrate-induced weakening of the TM7-TM1 hydrogen bond might be responsible for maintaining the differential tension on the unwound segments of TM1 and TM6 [13-18,20-22] (Fig. 4A-B). This would induce transitions to the next steps in the transport cycle [22]. Unexpectedly, recently solved human xCT/CD98hc structures showed a completely different mechanism that maintains the interactions between Tyr 281 (TM7) and both TM1 and TM6 in the substrate-bound conformation and the interaction with TM6 in the absence of substrate [19]. These differences, which would result in a different tension of the unwound segments of TM1 and TM6 upon substrate binding when compared to the rest of the solved HAT members, might reflect the distinct substrate-binding pose reported for xCT/CD98hc [19]. Whether the distinct calculated L-cystine-binding pose in xCT/CD98hc is an adaptation to the inwardly directed gradient of this substrate across the plasma membrane is at present unknown. It would be informative if this distinct binding pose is also present in $b^{0,+}$AT/rBAT, the other HAT that transports L-cystine.

A lysine residue within TM5, whose mutation in y^+LAT1/CD98hc (K191E) causes lysinuric protein intolerance [47] in in an equivalent position of the Na2 in the sodium-dependent transporters with APC-fold is of particular interest. It has been suggested to play a key role in the release of the substrate to the cytosol and in facilitating the outward-to-inward transition [22], thereby increasing apparent affinity for substrates at the extracellular face. This lysine residue mediates the coordination between TMs 1, 5 and 8 upon substrate binding and occlusion, and such coordination is key for function in the APC superfamily of transporters [22]. Thus, while this residue connects TM5 and TM1 in inward-open HAT and in bacterial LAT transporters (Fig. 4C) [13-15,17-22], rearrangements upon substrate binding (e.g., TM1a closing) results in TM1-TM5-TM8 coordination (Fig. 4D) [16,28]. Such

mediation can be observed in the inward occluded structures of bacterial GkApcT and human LAT1/CD98hc with the conserved lysine in this position (Fig. 4D) [16,28].

Additionally, molecular dynamics calculations in the prokaryotic LAT transporter BasC in the inward-facing conformation predicted that this lysine residue (Lys154 in TM5) would be the first interactor of the substrate on its way from the substrate-binding site to the cytosol [22]. These observations, together with the functional characterization of Lys 154 mutants, suggested that shifting the substrate from the binding site to contact Lys 154 might debilitate the connection of this residue with TM8, allowing the opening of TM1a and favoring transit to the inward-open facing conformation (Fig. 4E). Thus, in this proposed mechanism, the transition of BasC from a substrate-bound occluded conformation to an inward-open facing conformation would be facilitated by Lys 154. In this regard, Lys 154 would sustain V_{MAX} and the external K_M in the μM range by accelerating this otherwise limiting step of the transport cycle and play a key role in the establishment of an asymmetric substrate interaction at both sides of the plasma membrane [46].

Future perspective

The combination of structural, functional and computational analysis is paving the way to dissect mechanisms of substrate recognition and the molecular defects associated with HAT mutations that cause disease. Further structural studies are required to complete the structural landscape of the transport cycle of HATs. This knowledge will have a double value, namely understanding the transport mechanisms of these molecules and improving drug targeting of loss-of-function mutations in inherited diseases and the overexpression of HATs in cancer.

Acknowledgments. We are very grateful to Professor Simon Newstead, and to Dr Yongchan Lee and Professor Shushi Nagamori for early access to the atomic coordinates of glutamate-bound human xCT/CD98hc and ovine $b^{0,+}$AT/rBAT structures, respectively. Work on HATs is currently supported by a coordinated “La Caixa” Foundation Grant LCF/PR/HR20/52400017 to M.P. and O.L. Work at in Dr. Palacín’s group is also supported by the Spanish MCIU/AEI (AEI/10.13039/501100011033) Grant RTI2018-094211-B-100-ERDF-UE cofunded, La Maratò-TV3 Grant 202025-31, and Grant 2017 SGR 961 awarded by the

Government of Catalonia. Work at in Dr. Llorca´s group is also supported by the Spanish MCIU/AEI AEI/10.13039/501100011033-Grant PID2020-114429RB-I00, and ERDF-UE cofunded Grants Y2018/BIO4747 and P2018/NMT4443 from the Autonomous Region of Madrid. We gratefully acknowledge institutional funding from the AEI Centers of Excellence “Severo Ochoa” CEX2019-000891-S and CEX2019-000913-S. IRB Barcelona is a member of the CERCA system of the Catalonia Government. P.B. is supported by a CIBERER. J.R. is a Severo Ochoa Fellow.

Figure legends.

Figure 1. Molecular architecture of HATs. A) Cryo-EM atomic structure of human LAT2/CD98hc (PDB 7B00) [18]. CD98hc is shown in pink. The LAT2 structure is color coded as a rainbow (dark blue, cyan, green, yellow, and red) from the N to the C terminus. Detergent digitonin, occupying a cholesterol-binding site, is shown in dark purple. B) Cryo-EM volume of the $b^{0,+}$AT/rBAT superdimer (left) (PDB 6Li9) [15]. rBAT molecules are colored to distinguish protein domains [N-terminus and TM1’ (gray), and the extracellular domains A (blue), B (pink) and C (green)]. $b^{0,+}$AT subunits are color coded as a rainbow (dark blue, cyan, green, yellow, and red) from the N to the C terminus. $b^{0,+}$AT/rBAT heterodimer (right). Residues involved in the formation of superdimers, all located in the rBAT ectodomain, are highlighted (spheres), blue for domain A and pink for domain B. Ca^{2+} atom in the rBAT ectodomain of each protomer (green sphere). Plasma membrane limits have been estimated with the ppm server (https://opm.phar.umich.edu/ppm_server).

Figure 2. Location of cystinuria mutations of rBAT causing biogenesis defects. A) Leu 89 (highlighted in spheres) is located towards the N-terminus of TM1’ (gray) just before the segment interacting with TM4 of $b^{0,+}$AT and close to a conserved cholesterol (dark-purple)-binding site. Another cholesterol molecule (dark-purple) is shown in the back of $b^{0,+}$AT. This cholesterol molecule interacts with TM5. Atom coordinates corresponds to ovine $b^{0,+}$AT/rBAT (PDBID 7nf8) [20]. B) Thr 216 (highlighted in spheres) is located near the Ca^{2+} atom (green sphere) within the interface of subdomains BI and BII (pink) of the extracellular domain of rBAT. Ca^{2+} -interacting residues are highlighted (sticks), as well as nearby residues in domain A (blue) and B (pink) involved in superdimer formation. Figure generated

from PDB 6YUZ [17]. C) Arg 365 (highlighted in sticks with C atoms in orange) is located in helix α4 of domain A, with atoms at H bond distance from atoms of Val 361. The contiguous residue Arg 362 is at H bond distance of Asp 359 (C atoms in gray) in the other rBAT protomer (gray). Highlighted residues D369, M395, F401 and I402 are also interacting with the other rBAT protomer. D) Met 216 (spheres) is located at the interface between domain A and C of the ectodomain of rBAT. The intracatenary disulfide bridge Cys571–Cys666 (yellow) and the N-glycosylated Asn 575 (NAG in orange) are highlighted. PDB 6LI9 [15] was used in Figures C and D. Plasma membrane limits have been estimated with the ppm server (https://opm.phar.umich.edu/ppm_server).

Figure 3. The substrate-binding site of human LATs. A) Solved structures within the transport cycle of the light subunits of HATs and bacterial BasC and ApcT. This transport cycle corresponds to a mechanism of obligatory exchange of substrates, which is the case for HATs with the exception of xCT that shows also a facilitated diffusion mechanism of transport [2]. Structures in outward-facing conformation are still missing; red dot denotes substrate. The occluded structures of human LAT1 and bacterial GkApcT corresponds to variants more open to the extracellular side and to the cytosol respectively. The structures shown corresponds to the transporters highlighted in bold. PDBID of representative structures are shown between parentheses. B) L-leucine-bound human LAT2 (PDB 7CMI) [13]. C) L-arginine-bound human $b^{0,+}$AT (PDB 6LI9) [15]. D) L-glutamate-bound and human apo (only TM8 colored in gray is shown for the apo structure) xCT (PDB 7P9U) [19]. Transmembrane domains (TMs) of substrate-bound LATs (B-D) are color coded (TM1, blue; TM3, cyan; TM6, green; TM8, orange). Binding of L-glutamate refolds the unwound segment of TM8 of xCT. In the three panels, substrates (sticks and spheres) are colored with C atoms in light gray, and O and N atoms in red and blue respectively. Protein residues interacting with substrates are highlighted in sticks with C atoms colored according with TM, and O and N atoms in red and blue respectively. Hydrogen bonds of substrates with transporter residues are indicated (black lines).

Figure 4. Structural bases for the asymmetric interaction of LATs with substrates. The fully conserved residues Tyr 289 (TM7) and Lys 204 (TM5) (human LAT1 numbering) underlie the asymmetric interaction of LATs with substrates at both sides of the plasma

membrane [22]. A) Tyr 289 interacts with unwound segments of TM1 and TM6 in the apo inward-facing conformation (PDBID 6irs) [14], whereas in B) the BCH-bound inward-facing conformation interacts only with TM6 (PDBID 6irt) [14]. In A and B only TM1, 6 and 7 are depicted for clarity. C) Lys 204 interacts with Ile 64 (TM1 unwound) in the 2-aminobicyclo-(2,2,1)-heptane-2-carboxylic acid (BCH)-bound inward-facing conformation (PDBID 6irt), whereas in D) in the 3,5-diiodo-L-tyrosine (diiodo-Tyr)-bound occluded conformation, Lys 204 also interacts with Ser 334 in TM8 (PDBID 7dsq) [16]. In C and D only TM1, 5 and 8 are depicted for clarity. The C, O and N atoms of the highlighted residues are colored as the corresponding TMs, and in red and blue, respectively. BCH and diiodo-Tyr (sticks) are colored with C atoms in gray, and O and N atoms in red and blue respectively. Hydrogen bonds of substrates with transporter residues are indicated (black lines). E) Hypothetical model for the role of the conserved Lys residue in TM5 in the transport cycle of the light subunits of HAT. The model propose that shifting the amino acid substrate (AA) from the binding site (unwound segments of TM1 and TM6) to Lys 204 (human LAT1 numbering) would debilitate H bonds of the ε-amine group of this residue with Ser 334 facilitating the opening of the cytosolic gate (tilting of TM1a and the neighbor TM6b). Lys 204 is located in TM5, which TM is not depicted for clarity. In this model, the equilibrium would be displaced towards the opening of the cytosolic gate (red arrows) and Lys 204 would facilitate these opening to release the AA to the cytosol. In this way Lys 204 would support V_{MAX} and drive extracellular K_M of substrates to low μM values. Black lines indicate H bonds of Lys 204 with Ile 64 and/or Gly 61 in TM1a and Ser 334 in TM8. The cytosolic-gate occluded and the cytosolic-gate open models are based on the human LAT1 (PD ID: 7DSQ) bound to the inhibitor 3,5 diiodo tyrosine) and human LAT1 (PDB ID: 6IRT) bound to the substrate BCH respectively. Similar H-bonds of the conserved Lys in TM5 with TM1a and TM8 residues in the conformations of the substrate vestibule occluded or open to the cytosol are observed in all the solved structure of all mammalian HATs and bacterial BasC and GkApct.

References

1. Gauthier-Coles G, Vennitti J, Zhang Z, Comb WC, Xing S, Javed K, Bröer A, Bröer S: **Quantitative modelling of amino acid transport and homeostasis in mammalian cells**. *Nat Commun* 2021, **12**:5282.
2. Fotiadis D, Kanai Y, Palacín M: **The SLC3 and SLC7 families of amino acid transporters**. *Mol Aspects Med* 2013, **34**:139-158.
3. Fairweather SJ, Shah N, Bröer S: **Heteromeric Solute Carriers: Function, Structure, Pathology and Pharmacology**. *Adv Exp Med Biol* 2021, **21**:13-127.

4. Colas C: **Toward a Systematic Structural and Functional Annotation of Solute Carriers Transporters-Example of the SLC6 and SLC7 Families**. *Front Pharmacol* 2020, **11**:1229.
5. Tărlungeanu DC, Deliu E, Dotter CP, Kara M, Janiesch PC, Scalise M, Galluccio M, Tesulov M, Morelli E, Sonmez FM, et al.: **Impaired Amino Acid Transport at the Blood Brain Barrier Is a Cause of Autism Spectrum Disorder**. *Cell* 2016, **167**:1481-1494.e1418.
6. Espino Guarch M, Font-Llitjós M, Murillo-Cuesta S, Errasti-Murugarren E, Celaya AM, Girotto G, Vuckovic D, Mezzavilla M, Vilches C, Bodoy S, et al.: **Mutations in L-type amino acid transporter-2 support SLC7A8 as a novel gene involved in age-related hearing loss**. *Elife* 2018, **7**.
7. Xiong G, Liu C, Yang G, Feng M, Xu J, Zhao F, You L, Zhou L, Zheng L, Hu Y, et al.: **Long noncoding RNA GSTM3TV2 upregulates LAT2 and OLR1 by competitively sponging let-7 to promote gemcitabine resistance in pancreatic cancer**. *J Hematol Oncol* 2019, **12**:97.
8. Koppula P, Zhuang L, Gan B: **Cystine transporter SLC7A11/xCT in cancer: ferroptosis, nutrient dependency, and cancer therapy**. *Protein Cell* 2021, **12**:599-620.
9. Kanai Y: **Amino acid transporter LAT1 (SLC7A5) as a molecular target for cancer diagnosis and therapeutics**. *Pharmacol Ther* 2021, 10.1016/j.pharmthera.2021.107964:107964.
10. Uno Y, Coyle JT: **Glutamate hypothesis in schizophrenia**. *Psychiatry Clin Neurosci* 2019, **73**:204-215.
11. Sakimura K, Nakao K, Yoshikawa M, Suzuki M, Kimura H: **A novel Na(+) -Independent alanine-serine-cysteine transporter 1 inhibitor inhibits both influx and efflux of D-Serine**. *J Neurosci Res* 2016, **94**:888-895.
12. Rosenberg D, Artoul S, Segal AC, Kolodney G, Radzishevsky I, Dikopoltsev E, Foltyn VN, Inoue R, Mori H, Billard JM, et al.: **Neuronal D-serine and glycine release via the Asc-1 transporter regulates NMDA receptor-dependent synaptic activity**. *J Neurosci* 2013, **33**:3533-3544.
13. Yan R, Zhou J, Li Y, Lei J, Zhou Q: **Structural insight into the substrate recognition and transport mechanism of the human LAT2-4F2hc complex**. *Cell Discov* 2020, **6**:82.
14. Yan R, Zhao X, Lei J, Zhou Q: **Structure of the human LAT1-4F2hc heteromeric amino acid transporter complex**. *Nature* 2019, **568**:127-130.
15. Yan R, Li Y, Shi Y, Zhou J, Lei J, Huang J, Zhou Q: **Cryo-EM structure of the human heteromeric amino acid transporter b(0,+)AT-rBAT**. *Sci Adv* 2020, **6**:eaay6379.
16. Yan R, Li Y, Müller J, Zhang Y, Singer S, Xia L, Zhong X, Gertsch J, Altmann KH, Zhou Q: **Mechanism of substrate transport and inhibition of the human LAT1-4F2hc amino acid transporter**. *Cell Discov* 2021, **7**:16.
17. Wu D, Grund TN, Welsch S, Mills DJ, Michel M, Safarian S, Michel H: **Structural basis for amino acid exchange by a human heteromeric amino acid transporter**. *Proc Natl Acad Sci U S A* 2020, **117**:21281-21287.
18. Rodriguez CF, Escudero-Bravo P, Díaz L, Bartoccioni P, García-Martín C, Gilabert JG, Boskovic J, Guallar V, Errasti-Murugarren E, Llorca O, et al.: **Structural basis for substrate specificity of heteromeric transporters of neutral amino acids**. *Proc Natl Acad Sci U S A* 2021, **118**.
19. Parker JL, Deme JC, Kolokouris D, Kuteyi G, Biggin PC, Lea SM, Newstead S: **Molecular basis for redox control by the human cystine/glutamate antiporter system xc()**. *Nat Commun* 2021, **12**:7147.
20. Lee Y, Wiriyasermkul P, Moriyama S, Mills DJ, Kühlbrandt W, Nagamori S: **Ca²⁺-mediated higher-order assembly of b^{0,+}AT–rBAT is a key step for system b^{0,+} biogenesis and cystinuria**. *bioRxiv* 2021, 10.1101/2021.05.06.443019:2021.2005.2006.443019.

21. Lee Y, Wiriyasermkul P, Jin C, Quan L, Ohgaki R, Okuda S, Kusakizako T, Nishizawa T, Oda K, Ishitani R, et al.: **Cryo-EM structure of the human L-type amino acid transporter 1 in complex with glycoprotein CD98hc**. *Nat Struct Mol Biol* 2019, **26**:510-517.
22. Errasti-Murugarren E, Fort J, Bartoccioni P, Díaz L, Pardon E, Carpena X, Espino-Guarch M, Zorzano A, Ziegler C, Steyaert J, et al.: **L amino acid transporter structure and molecular bases for the asymmetry of substrate interaction**. *Nat Commun* 2019, **10**:1807.
23. Janeček Š, Gabriško M: **Remarkable evolutionary relatedness among the enzymes and proteins from the α-amylase family**. *Cell Mol Life Sci* 2016, **73**:2707-2725.
24. Yamashita A, Singh SK, Kawate T, Jin Y, Gouaux E: **Crystal structure of a bacterial homologue of Na+/Cl--dependent neurotransmitter transporters**. *Nature* 2005, **437**:215-223.
25. Forrest LR, Rudnick G: **The rocking bundle: a mechanism for ion-coupled solute flux by symmetrical transporters**. *Physiology (Bethesda)* 2009, **24**:377-386.
26. Drew D, Boudker O: **Shared Molecular Mechanisms of Membrane Transporters**. *Annu Rev Biochem* 2016, **85**:543-572.
27. Stolzenberg S, Li Z, Quick M, Malinauskaite L, Nissen P, Weinstein H, Javitch JA, Shi L: **The role of transmembrane segment 5 (TM5) in Na2 release and the conformational transition of neurotransmitter:sodium symporters toward the inward-open state**. *J Biol Chem* 2017, **292**:7372-7384.
28. Jungnickel KEJ, Parker JL, Newstead S: **Structural basis for amino acid transport by the CAT family of SLC7 transporters**. *Nat Commun* 2018, **9**:550.
29. Jumper J, Evans R, Pritzel A, Green T, Figurnov M, Ronneberger O, Tunyasuvunakool K, Bates R, Žídek A, Potapenko A, et al.: **Highly accurate protein structure prediction with AlphaFold**. *Nature* 2021, **596**:583-589.
30. Fort J, de la Ballina LR, Burghardt HE, Ferrer-Costa C, Turnay J, Ferrer-Orta C, Usón I, Zorzano A, Fernández-Recio J, Orozco M, et al.: **The structure of human 4F2hc ectodomain provides a model for homodimerization and electrostatic interaction with plasma membrane**. *J Biol Chem* 2007, **282**:31444-31452.
31. Fernández E, Jiménez-Vidal M, Calvo M, Zorzano A, Tebar F, Palacín M, Chillarón J: **The structural and functional units of heteromeric amino acid transporters. The heavy subunit rBAT dictates oligomerization of the heteromeric amino acid transporters**. *J Biol Chem* 2006, **281**:26552-26561.
32. Bartoccioni P, Rius M, Zorzano A, Palacín M, Chillarón J: **Distinct classes of trafficking rBAT mutants cause the type I cystinuria phenotype**. *Hum Mol Genet* 2008, **17**:1845-1854.
33. Bauch C, Verrey F: **Apical heterodimeric cystine and cationic amino acid transporter expressed in MDCK cells**. *Am J Physiol Renal Physiol* 2002, **283**:F181-189.
34. Feliubadaló L, Font M, Purroy J, Rousaud F, Estivill X, Nunes V, Golomb E, Centola M, Aksentijevich I, Kreiss Y, et al.: **Non-type I cystinuria caused by mutations in SLC7A9, encoding a subunit (bo,+AT) of rBAT**. *Nat Genet* 1999, **23**:52-57.
35. Reig N, Chillarón J, Bartoccioni P, Fernández E, Bendahan A, Zorzano A, Kanner B, Palacín M, Bertran J: **The light subunit of system b(o,+) is fully functional in the absence of the heavy subunit**. *Embo j* 2002, **21**:4906-4914.
36. Rius M, Chillarón J: **Carrier subunit of plasma membrane transporter is required for oxidative folding of its helper subunit**. *J Biol Chem* 2012, **287**:18190-18200.
37. Rius M, Sala L, Chillarón J: **The role of N-glycans and the C-terminal loop of the subunit rBAT in the biogenesis of the cystinuria-associated transporter**. *Biochem J* 2016, **473**:233-244.
38. Rosell A, Meury M, Álvarez-Marimon E, Costa M, Pérez-Cano L, Zorzano A, Fernández-Recio J, Palacín M, Fotiadis D: **Structural bases for the interaction and stabilization of the human**

amino acid transporter LAT2 with its ancillary protein 4F2hc. *Proc Natl Acad Sci U S A* 2014, **111**:2966-2971.
39. Rajan DP, Kekuda R, Huang W, Devoe LD, Leibach FH, Prasad PD, Ganapathy V: **Cloning and functional characterization of a Na(+)-independent, broad-specific neutral amino acid transporter from mammalian intestine**. *Biochim Biophys Acta* 2000, **1463**:6-14.
40. Matsuo H, Kanai Y, Tokunaga M, Nakata T, Chairoungdua A, Ishimine H, Tsukada S, Ooigawa H, Nawashiro H, Kobayashi Y, et al.: **High affinity D- and L-serine transporter Asc-1: cloning and dendritic localization in the rat cerebral and cerebellar cortices**. *Neurosci Lett* 2004, **358**:123-126.
41. Kanai Y, Segawa H, Miyamoto K, Uchino H, Takeda E, Endou H: **Expression cloning and characterization of a transporter for large neutral amino acids activated by the heavy chain of 4F2 antigen (CD98)**. *J Biol Chem* 1998, **273**:23629-23632.
42. Pfeiffer R, Loffing J, Rossier G, Bauch C, Meier C, Eggermann T, Loffing-Cueni D, Kühn LC, Verrey F: **Luminal heterodimeric amino acid transporter defective in cystinuria**. *Mol Biol Cell* 1999, **10**:4135-4147.
43. LeVine MV, Terry DS, Khelashvili G, Siegel ZS, Quick M, Javitch JA, Blanchard SC, Weinstein H: **The allosteric mechanism of substrate-specific transport in SLC6 is mediated by a volumetric sensor**. *Proc Natl Acad Sci U S A* 2019, **116**:15947-15956.
44. Focht D, Neumann C, Lyons J, Eguskiza Bilbao A, Blunck R, Malinauskaite L, Schwarz IO, Javitch JA, Quick M, Nissen P: **A non-helical region in transmembrane helix 6 of hydrophobic amino acid transporter MhsT mediates substrate recognition**. *Embo j* 2021, **40**:e105164.
45. Sato H, Tamba M, Kuriyama-Matsumura K, Okuno S, Bannai S: **Molecular cloning and expression of human xCT, the light chain of amino acid transport system xc**. *Antioxid Redox Signal* 2000, **2**:665-671.
46. Meier C, Ristic Z, Klauser S, Verrey F: **Activation of system L heterodimeric amino acid exchangers by intracellular substrates**. *Embo j* 2002, **21**:580-589.
47. Sperandeo MP, Andria G, Sebastio G: **Lysinuric protein intolerance: update and extended mutation analysis of the SLC7A7 gene**. *Hum Mutat* 2008, **29**:14-21.

Figure 1

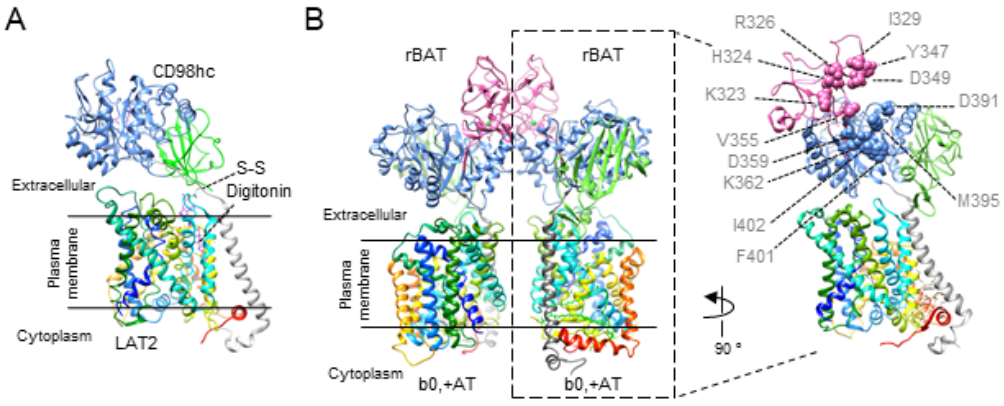

Figure 2

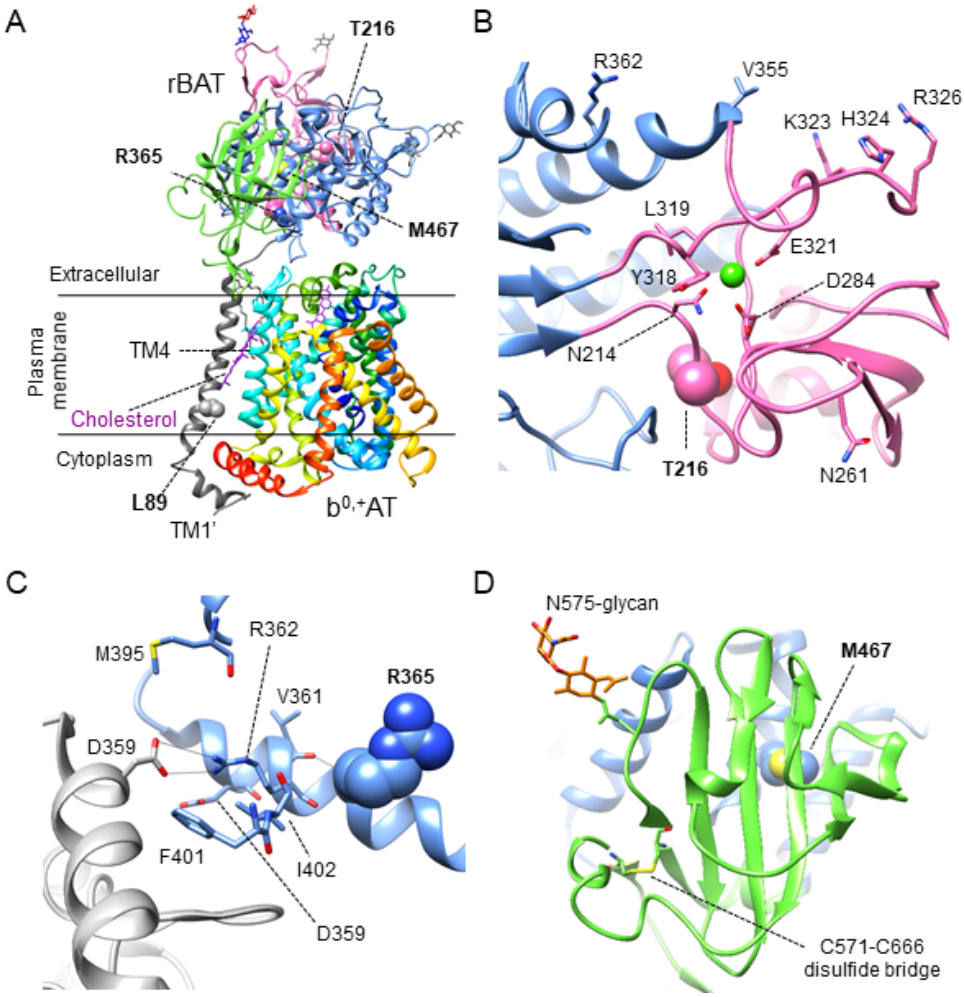

524

Figure 3

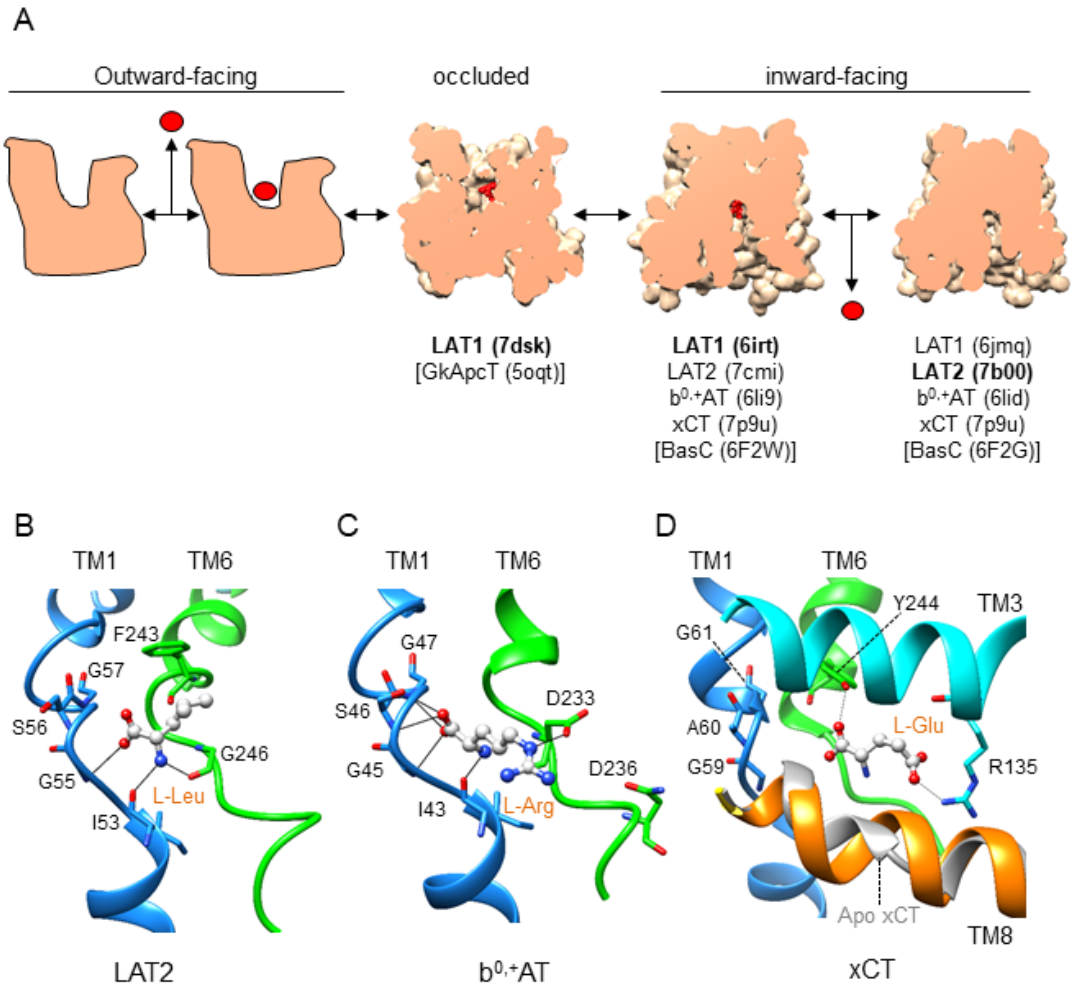

525

526

527 Figure 4

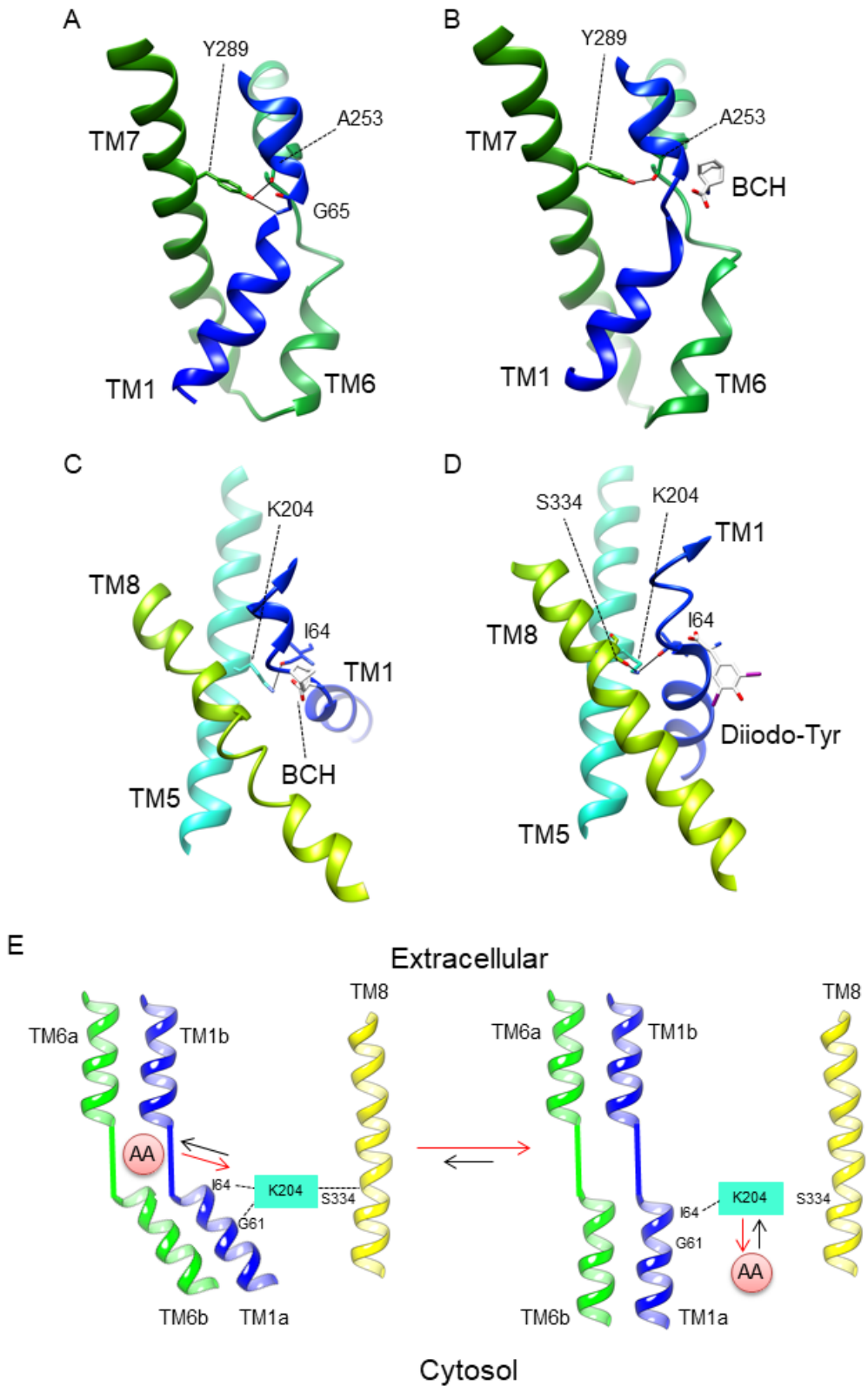

528